4　病型

一九九五年、Birdらは初期と後期にわけて分類しました。

1、初期加齢黄斑症

網膜の下にドルーゼンという沈着物や、網膜と脈絡膜の間に存在する「網膜色素上皮細胞」という細胞の異常がみられるものです。軽いゆがみの自覚はありますが、視力は良いことが多いです。

2、後期加齢黄斑症

いわゆる加齢黄斑変性です。これはさらに

A：脈絡膜新生血管から出血、水たまりをおこす滲出型 exudative type

B：脈絡膜新生血管が関与せず、網膜色素上皮細胞や脈絡膜の毛細血管の萎縮をきたす萎縮型 atrophic type

に分類されます。

滲出型は視力低下が高度であることが多く、臨床的に重要視されています。

一方、萎縮型は、治療法はありませんが、進行は年単位の緩やかな場合が多いのです。

5　検査・診断

眼科を受診していただき、まず行うのが、視力、眼圧、眼底検査などの一般的なものです。これは一般の開業医でも十分に行える検査です。

ここで加齢黄斑変性がみつかった場合はフルオレセイン蛍光眼底造影、インドシアニングリーン蛍光眼底造影といった、血管を造影する検査を行い、さらに光干渉断層計で網膜の断面図を描出します。これらの検査によって病型の把握、脈絡膜新生血管の場所、大きさ、網膜剥離の有無、出血の有無、出血の量、周囲の健常な組織の状態を見ていくわけです。この検査になると、ある程度大きな病院でないと、設備が整っていないので受けることができません。

6　治療

さて、実際に、加齢黄斑変性の診断を受けた場合、どのような治療を受けることになるのでしょうか。加齢黄斑変性の各々の病型で説明していきましょう。

1、初期加齢黄斑症：

このタイプは変性がわずかであり、ちょっと鈍感な方なら発症していても気づかないこともあります。視力がよいので、治療によってかえって正常網膜を障害

することもありますので、治療を行いません。後期加齢黄斑症への移行を早くとらえるためにも、定期的な経過観察が必要になります。後期加齢黄斑症の滲出型へ移行した場合、発症からの時期が早く網膜の変性が進行していない症例がよい治療の適応となるからです。

2、後期加齢黄斑症　萎縮型：

加齢によってじわじわと進行する細胞レベルの変化ですので、治療はできないのです。このじわじわとした進行を少しでも遅らせるためにアメリカで開発されたサプリメント（商品名：オキュバイト）はアメリカでは有意に萎縮型の加齢黄斑変性の進行を抑えることが出来た、との報告があり、我々も萎縮型の患者さんや片眼に発症している方の反対眼（正常眼）の発症予防にお勧めしています。

3、後期加齢黄斑症　滲出型：

一度、新生血管からの水たまりや出血を掃除機のようなもので吸い取って、元通りの網膜に戻すことができれば視力は回復するはずです。しかし残念なことに、黄斑という部位は繊細な神経細胞の集まりであり、扱えば扱うだけダメージも与えてしまうことになりかねません。つまり、落ちた視力を元通りにもどすという治療はできないのです。では、治療は何のためにするのでしょうか。この病気の厄介者である新生血管が残っている限り、何度も出血や水たまりを繰り返し、確実に悪化への一途をたどります。それを少しでも食い止めるために新生血管をつぶすことが治療の中心になるのです。新生血管の位置によって治療法は大きく二通りのレーザー治療に分けられます。

・中心窩外にある新生血管

新生血管が黄斑の中心（中心窩）や、その近傍に及んでいない場合は、レーザー光凝固が第一選択となります。新生血管を周囲の健常組織ごと凝固するため、結果として凝固点は絶対見えない部分（絶対暗点）として残るため、中心窩に新生血管がある場合は行うことができません。通常外来での治療が可能で、レーザー処置は痛みを伴いません。治療直後に帰宅することができます。

・中心窩にある新生血管

脈絡膜新生血管が中心窩に及んでいる場合は中心窩を強く傷害するような治療は選択できません。現在我が国ではverteporfin（二〇〇四年認可）という薬剤を用いた光線力学的療法（photodynamic therapy: PDT）が第一選択となっています。光線力学的療法は薬剤投与、非熱レーザー照射の二段階で行われます。まずverteporfinの静脈内投与を行い、verteporfinを新生

血管に取り込ませます。次に投与開始から一五分後に波長六八九㎚の非熱レーザーを照射することで光化学反応をおこし、血管内皮細胞を傷害し、新生血管を閉塞させるのです。周囲の組織に障害を与えずに新生血管のみを退縮させることができます。通常のレーザー治療同様、全く痛みを伴いませんが、光感受性物質が体の中に入っている五日間は直射日光にあたってはいけないため、入院して施行する施設もあります。再治療は三ヶ月毎に何度でも行うことができますが、変性・線維化した病変には無効です。

いずれの場合でも黄斑が萎縮または線維化を来している場合は残念ながら治療の効果は期待できません。他の多くの疾患同様、早期の発見、適応に応じた治療、が重要なのです。

7　新しい治療

抗血管新生薬の開発が現在進行しています。海外では眼内（硝子体内）へ注入する二種類の薬剤が認可されており、国内でも臨床試験が行われている状況です。これらの薬剤は血管内皮増殖因子（vascular endothelial growth factor:VEGF）という血管系が成長するのに必要な因子の働きを阻害する抗血管内皮増殖因子薬です。海外治験ではいずれの薬剤も光線力学的療法と同等かそれ以上の効果が認められています。

加齢黄斑変性に対する研究は確実に進歩してきているのです。

（九州大学大学院医学研究院眼科教授・九大・医・昭50）

Protective Role for CD1d-Reactive Invariant Natural Killer T Cells in Cauterization-Induced Corneal Inflammation

Toru Oshima,[1] Koh-Hei Sonoda,[1] Shintaro Nakao,[1] Kuniaki Hijioka,[1] Masaru Taniguchi,[2] and Tatsuro Ishibashi[1]

Purpose. Corneal inflammation can be induced by various stimuli, such as chemical burns, trauma, and acute bacterial infection, and directly impairs visual acuity. Natural killer T (NKT) cells belong to a specialized population of leukocytes that coexpress the T-cell receptor and NK markers. This study examined the role of CD1d-reactive invariant NKT cells in cauterization-induced acute corneal inflammation.

Methods. The corneas of CD1d-knockout (KO) mice and Jα18-KO mice (both of which are NKT cell deficient) and control mice were cauterized with silver nitrate. Corneal edema and opacity were examined, and the phenotypes of the corneal-infiltrating cells were analyzed histologically at 24 hours and by flow cytometry at 96 hours. Reverse transcription–polymerase chain reaction (RT-PCR) was used to determine the expression of vascular endothelial growth factor (VEGF), interferon (IFN)γ, and tumor necrosis factor (TNF)α in the cauterized corneas.

Results. The CD1d-KO and Jα18-KO mice had significantly greater levels of corneal edema and opacity than did the control mice. Although the number of infiltrating cells was not significantly different at 96 hours, both groups of NKT cell-deficient mice demonstrated increased early neutrophil accumulation at 24 hours and early expression of VEGF, IFNγ, and TNFα. There was no difference in the level of VEGF-induced corneal neovascularization.

Conclusions. NKT cells appear to regulate the early accumulation of neutrophils, protect the cornea from excessive inflammation, and maintain corneal clarity. However, in this study, they did not affect the corneal revascularization process induced by VEGF. (*Invest Ophthalmol Vis Sci.* 2008;49:105–112) DOI:10.1167/iovs.07-0284

The eye is a specialized organ that is capable of limiting excessive inflammation to avoid loss of vision. This is known as immune privilege of the eye and is attributed to a variety of local factors, including the lack of lymphatic drainage,[1] Fas-ligand expression,[2] and multiple immunosuppressive factors in the aqueous humor.[3,4] Because the cornea is located at the front of the eye and is exposed to many dangerous stimuli, excessive reactive inflammation might directly induce irreversible opacity.[5,6] It is, therefore, important to elucidate the cellular and molecular mechanisms responsible for controlling inflammation to maintain the clarity of the cornea.

In general, nonspecific corneal inflammation is initiated by innate immunity.[7] The corneal expression of proinflammatory cytokines and chemokines in response to injury or infection leads to the recruitment of cells of the innate immune system. We previously demonstrated the critical role of neutrophils in experimental corneal inflammation.[8]

Natural killer T (NKT) cells belong to a specialized population of leukocytes that coexpress the T-cell receptor (TCR) αβ chain and NK markers,[9,10] and they are classified as mediators of the innate immune response. Approximately 85% of the mouse NKT cell population expresses a restricted TCR repertoire consisting of an invariant TCRα chain (Vα14 Jα18).[11,12] Similarly, human NKT cells express the invariant Vα24 JαQ TCR chain.[13] NKT cells are restricted by major histocompatibility complex (MHC) class I-like CD1d molecules,[14,15] and, because the CD1d molecule is also required for the development of NKT cells, CD1d-knockout (KO) mice selectively lack NKT cells.[16–18] The role of NKT cells in disease models has been reported in terms of tumor rejection,[19] abortion,[20] and infection.[21,22] Several reports also imply a role for NKT cells in preventing certain autoimmune diseases[23,24] and inducing transplantation tolerance.[25,26]

In addition to local mechanisms, ocular immune privilege is associated with the development of antigen-specific systemic immunologic tolerance. The mechanisms of ocular-type immunologic tolerance have been well studied in an experimental system, known as the anterior chamber-associated immune deviation (ACAID) animal model.[1] ACAID is a critically important dimension of the ability of the immune system to protect the eye from various types of inflammations, including postoperative injury. For example, a host bearing a long-term clear corneal allograft displays an antigen-specific downregulation of the delayed-type hypersensitivity response to donor alloantigens that is reminiscent of ACAID.[27] Sonoda et al.[28,29] demonstrated that CD1d-reactive NKT cells are critical for ACAID and transplantation tolerance after corneal allograft. Indeed, NKT cell-deficient mice failed to induce donor-specific tolerance and were unable to accept corneal grafts in the long term.[28]

In the present study, we developed a cauterization-induced corneal inflammation model and compared the extent of local inflammation between control mice and NKT cell-deficient mice to elucidate the role of NKT cells in nonspecific corneal inflammation.

Methods

Mice

Female mice (8–10 weeks old) were used in all experiments. C57BL/6 (B6) mice were obtained from SLC Japan (Shizuoka, Japan). CD1d-KO

From the [1]Department of Ophthalmology, Graduate School of Medical Science, Kyushu University, Fukuoka, Japan; and the [2]Laboratory for Immune Regulation, RIKEN Research Center for Allergy and Immunology, Kanagawa, Japan.

Supported in part by grants from the Ministry of Education, Science, Sports and Culture, Japan (C2 No.16571757: K-HS).

Submitted for publication March 8, 2007; revised August 18, 2007; accepted November 20, 2007.

Disclosure: **T. Oshima**, None; **K.-H. Sonoda**, None; **S. Nakao**, None; **K. Hijioka**, None; **M. Taniguchi**, None; **T. Ishibashi**, None

The publication costs of this article were defrayed in part by page charge payment. This article must therefore be marked "*advertisement*" in accordance with 18 U.S.C. §1734 solely to indicate this fact.

Corresponding author: Koh-Hei Sonoda, Department of Ophthalmology, Graduate School of Medical Sciences, Kyushu University, 3-1-1 Maidashi, Higashi-Ku, Fukuoka, Japan; sonodak@med.kyushu-u.ac.jp.

mice were generated in the Transgenic Facility of Harvard Medical School (Boston, MA) and were backcrossed to B6 mice for six generations.[29] Jα18-KO mice (NKT-KO mice) were generated at Chiba University (Chiba, Japan) and were backcrossed eight times to B6 mice.[19] All mice were maintained on food and water ad libitum until they reached the desired weight (20–24 g). All animals were treated humanely and were housed in specific pathogen-free conditions at Kyushu University (Japan). Treatment of the animals conformed to the ARVO Statement for the Use of Animals in Ophthalmic and Vision Research.

Induction and Evaluation of Corneal Inflammation

Corneal inflammation was induced as described previously.[30] The center of the right cornea of each mouse was cauterized with 1-mm diameter plastic sticks containing 0.4 g/mL silver nitrate. After 96 hours, corneal edema and opacity were evaluated by stereoscopic microscopy with a slit lamp. Cauterization and evaluation were performed in a masked fashion. Lesions were scored for corneal edema and opacity on scales of increasing severity from 0 to +4. For edema, the scores corresponded to the following descriptions: 0, completely normal cornea; +1, no evidence of ongoing edema, corneal thickness less than normal; +2, mild edema limited to the cauterized area, corneal thickness increased but less than two times that of the normal cornea; +3, severe edema limited to the cauterized area, corneal thickness more than two times that of the normal cornea; +4, extensive edema extended to the whole cornea, corneal perforation in some cases. For opacity, the scores corresponded to the following descriptions: 0, completely clear cornea; +1, slight opacity; +2, mild opacity, iris and lens visible; +3, severe opacity limited to the cauterized area, iris and lens invisible; +4, extensive opacity extended to the whole cornea.

Corneal neovascularization was evaluated according to length and extension and occurred in particular areas of the limbal vascular plexus where neovascularized contiguous limbal circumferential zones formed. Neovascularization often occurred in the total limbal vascular plexus in severely damaged corneas. Maximum vessel length was measured from the limbs toward the cauterized area within the total neovascular zones using a linear reticule through a slit lamp. To assess vessel extension, the central angle of each contiguous circumferential zone of neovascularization was measured with a 360° reticule. All results are expressed per cornea.

Reverse Transcription–Polymerase Chain Reaction

The right eyes were removed from mice ($n = 3$, pooled samples of three eyes) at 24, 48, and 96 hours after cauterization under deep anesthesia. Whole corneas, including neovascular invasion, were isolated and dissected. Total retinal messenger RNA (mRNA) was extracted (Trizol; Life Technologies, Grand Island, NY) and reverse transcribed (RT; Gene Amp PCR System 9600; Perkin-Elmer, Norwalk, CT). First-strand complementary DNA (cDNA) was synthesized using AMV reverse transcriptase (Boehringer Mannheim, Indianapolis, IN) according to the manufacturer's guidelines. Incubations were carried out for 10 minutes at 25°C and 60 minutes at 42°C, and reverse transcriptase (Boehringer Mannheim) was denatured at 99°C for 5 minutes before PCR amplification. PCR of the cDNAs was carried out in 20-μL volumes containing 10 pmol primer pair and 2 μL thermal cycling (LightCycler; Roche, Indianapolis, IN). In total, 30 amplification cycles were performed, and the PCR products were separated on 2% agarose gels. Band intensities were measured with an image sensor (Densitograph; Atto, Tokyo, Japan) with a computer-controlled display. Primers used in these experiments were as follows: β-actin, sense 5′-GTG GGC CGC TCT AGG CAC CAA-3′, antisense 5′-CTC TTT GAT GTC ACG CAC GAT TTC-3′ (product size, 539); VEGF, sense 5′-TTA CTG CTG TAC CTC CAC C-3′, antisense 5′-ACA GGA CGG CTT GAA GAT G-3′ (product size, 189 base pairs [bp]); tumor necrosis factor (TNF)α, sense 5′-GGC AGG TCT ACT TTG GAG TCA TTG-3′, antisense 5′-ACA TTC GAG GCT CCA GTG AAT TCG G-3′ (product size, 309 bp); interferon (IFN)γ, sense 5′-AGCGGCTGACTGAACTCAGATTGTAG-3′, antisense 5′-GTCA CAGTTTTCAGCTGTATAGGG-3′ (product size, 213 bp); and Vα14, sense 5′-GTTGTCCGTCAGGGAGAGAA-3′, antisense 5′-TCCCTAAG GCTGAACCTCTATC-3′ (product size, 268 bp).

mRNA Quantification by Reverse Transcription–Polymerase Chain Reaction

Total RNA was extracted from whole eyes 12 or 24 hours after photocoagulation (Trizol; Life Technologies). An aliquot (approximately 1 μg) of the total RNA was reverse-transcribed using a first-strand cDNA synthesis kit for RT-PCR (Roche Diagnostics) according to the manufacturer's instructions. The reverse-transcribed cDNAs were then subjected to real-time RT-PCR (SYBR Premix Ex Taq; TaKaRa Bio Inc., Otsu, Japan) and thermal cycling (LightCycler; Roche). Reaction conditions were as follows: denaturing at 95°C for 10 seconds followed by 40 cycles of denaturing at 95°C for 5 seconds and annealing and extending at 60°C for 20 seconds. The level of mRNA expression for *IL-18* was estimated from the fluorescence intensity relative to β-actin. Primers used were 5′-CTAAGCACAGCACGCTGCACA-3′ and 5′-AGG TATGACAATCAGCTGAGTCCC-3′ for Vα14, 5′-CCCTTTTGGGCCTAT GCAG-3′ and 5′-ATGCCTCGAAGAGTTTTGCAC-3′ for CXCR6, and 5′-GATGACCCAGATCATGTTTGA-3′ and 5′-GGAGAGCATAGCCCTCGTAG-3′ for β-actin. Each experiment was repeated at least twice, and representative data are shown.

Isolation of Corneal-Infiltrating Cells

Inflammatory cells were isolated from the corneas, as described for hepatic lymphocytes, with some modifications.[30] Three corneas were pooled to obtain enough viable cells for flow cytometry. Corneas were teased away with scissors and shaken at 37°C for 40 minutes with 0.5 mg/mL collagenase (Collagenase Type D; Boehringer Mannheim, Germany). Supernatants were collected, and viable cells were counted using trypan blue dye exclusion. Eighteen corneas were examined as six pooled samples of three individual eyes.

Antibodies and Reagents

The following reagents were used for flow cytometry: phycoerythrin (PE)-conjugated anti-CD11b monoclonal antibody (mAb; clone M1/70.15) and fluorescein isothiocyanate (FITC)-conjugated anti-F4/80 mAb (clone A3-1) from Caltag Laboratory, Inc. (San Francisco, CA); FITC-conjugated anti-Gr-1 mAb (clone RB6-8C5), Cy-Chrome 5-conjugated anti-TCRβmAb (H57-597), PE-conjugated CD4 (RM4-5) and propidium iodide staining solution from BD Bioscience (San Jose, CA); and FITC-conjugated anti-mouse 7/4 mAb from Cedarlane Laboratory (Ontario, Canada). Antibodies used for labeling sections were anti F4/80 mAb (clone A3-1; Serotec, Oxford, UK) and Cy5-conjugated goat anti-rat immunoglobulin G (IgG) antibody (Zymed Laboratory, San Francisco, CA).

Flow Cytometry

Corneal-infiltrating cells were adjusted to the required concentrations for two-color labeling. Macrophages within the intraocular infiltrate were identified by double labeling with PE-anti-CD11b mAb and FITC-conjugated anti-F4/80 mAb. Cells stained with PE-anti-CD11b mAb and FITC-anti-7/4 mAb were identified as neutrophils. Analysis was performed on a flow cytometer (EPICS XL; Beckman Coulter, Mannheim, Germany) with data analysis software (FlowJo; Tree Star, San Carlos, CA). Propidium iodide staining was used to discriminate dead cells. The numbers of macrophages and neutrophils infiltrating the cornea were calculated from the percentage of each population measured by flow cytometry, and the total number of viable cells was counted by trypan blue dye exclusion. The gate within which the F4/80+ and 7/4+ cells were counted was set using an isotype-matched control antibody (FITC-conjugated rat IgG2b; Caltag Laboratory, Inc.,

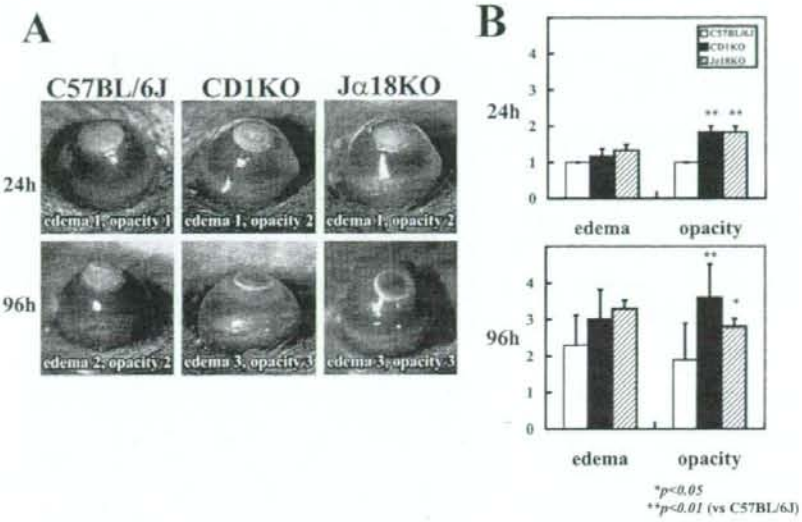

FIGURE 1. Corneal inflammation in NKT-deficient mice. Corneas (n = 10) were cauterized with silver nitrate in control (C57BL/6J) and NKT cell-deficient (CD1d KO and Jα18 KO) mice. Corneal edema and opacity were examined at 24 hours and 96 hours after cauterization (**A**) and were scored according to severity (**B**). $^{*}P < 0.05$, $^{**}P < 0.01$, compared with control mice. The experiment was performed three times with similar results.

San Francisco, CA). CD11b-F4/80− (double negative) cells, possibly containing keratocytes,[31] constantly made up less than 2% to 3% of the total isolated viable cells.

Corneal Micropocket Assay

The corneal micropocket assay and the quantification of corneal neovascularization were performed as described previously.[32,33] Briefly, 0.3 μL poly(hydroxyethyl) methacrylate pellets (Hydron; Interferon Sciences, New Brunswick, NJ) containing 30 ng human or murine IL-1β or 200 ng murine VEGF (493-MV; R&D Systems, Minneapolis, MN) were prepared and implanted into the corneas of C57BL/6 mice, CD1d-KO mice, or Jα18-KO mice. After implantation, ofloxacin eyedrops (Santen Pharmaceuticals, Osaka, Japan) were applied to each eye to prevent infection. Six days after implantation, digital images of the corneal vessels were obtained and recorded (Viewfinder 3.0; Pixera, Los Gatos, CA), with standardized illumination and contrast, and were saved to disks. Quantitative analysis of neovascularization was performed using digital imaging software (Image, version 4.0.2; Scion Corp., Frederick, MD).

Histologic Examination

Freshly enucleated eyes were fixed in 10% paraformaldehyde and embedded in paraffin. Sections (4 μm) were then prepared and were stained with hematoxylin and eosin solution. The numbers of neutrophils and macrophages were counted under the microscope in three independent visual fields (magnification, ×200) in the cornea and in the anterior chamber, and the average was calculated.

Statistical Analysis

Significant differences in the grade of corneal inflammation were assessed using the Student's t-test. $P \leq 0.05$ was considered significant.

RESULTS

NKT-Deficient Mice Showed Augmentation of Corneal Edema and Opacity

Initially, we examined corneal inflammation in two independently derived NKT cell-deficient mice (CD1d KO and Jα18 KO). At 24 hours after cauterization, opacity scores had increased in both types of NKT-deficient mice, though the edema scores were not significantly different. At 96 hours after cauterization, both types of NKT-deficient mice showed significant increases in opacity and edema compared with control B6 mice (Figs. 1A, 1B). No differences were observed in corneal edema or opacity between CD1d-KO mice and Jα18-KO mice during the entire experiment.

NKT-Deficient Mice Enhanced the Early Production of VEGF, IFNγ, and TNFα

To understand the functional changes that occurred in the cornea after cauterization in NKT cell-deficient mice, we examined VEGF, IFNγ, and TNFα expression at multiple time points (24, 48, and 96 hours) using RT-PCR. VEGF expression peaked 24 hours after cauterization and regressed by 48 hours in NKT cell-deficient mice (Fig. 2). By contrast, VEGF expression peaked at 48 hours in control mice. Both types of NKT cell-deficient mice expressed higher levels of IFNγ and TNFα at 24 and 48 hours compared with control mice.

Early Infiltration of Neutrophils into the Cornea Was Observed Histologically

We next examined the phenotype of corneal infiltrating cells during the early phase. We have previously demonstrated a role for neutrophils as the final effector cells mediating cauterization-induced corneal inflammation.[8] In addition, F4/80+ macrophages may contribute to the activation of accumulating neutrophils during inflammation.[30] We thus examined the numbers of corneal neutrophils and macrophages. The severity of corneal inflammation was insufficient to achieve this by flow cytometry, and it was difficult to obtain enough corneal-infiltrating cells for accurate analysis. Therefore, we evaluated early changes of the cornea by histologic analysis.

As shown in Figure 3, marked infiltration of viable neutrophils, with clover-like nuclei (Fig. 3B), was observed in the corneas and anterior chambers of both types of NKT cell-deficient mice but not in control mice. The thickness of the cauterized area was prominently increased in Jα18-KO mice (Fig. 3B).

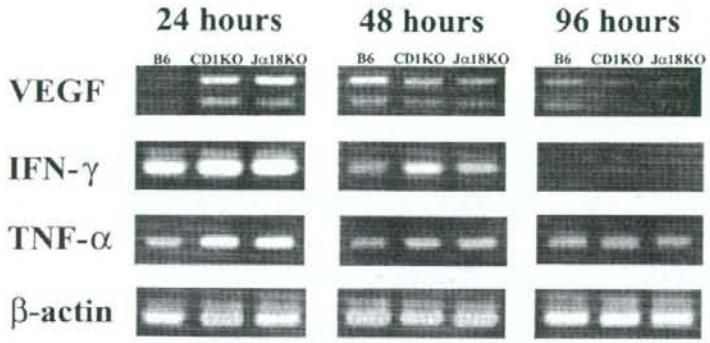

FIGURE 2. VEGF, TNFα, and IFNγ expression after cauterization. The right eyes (n = 3) were removed at 24, 48, and 96 hours after cauterization from control (B6) and NKT cell-deficient (CD1 KO and Jα18 KO) mice, and total corneal mRNA was extracted for the examination of VEGF, TNFα, and IFNγ expression. Three corneas were pooled to obtain sufficient mRNA. The experiment was performed three times with similar results.

Recruited Neutrophils and Macrophages Did Not Decrease in Number in NKT-Deficient Mice during the Later Phase

Next we examined the number of corneal-recruiting neutrophils and macrophages by flow cytometry during the effector phase (96 hours). Figure 4A (left panel) demonstrates the typical flow data of macrophages and neutrophils in B6 mice, which can clearly be discriminated by F4/80 and 7/4 antibody staining. Although the corneal edema and opacity scores were significantly increased at 96 hours, the numbers of ocular infiltrating neutrophils and macrophages did not increase (Fig. 4A, right panel). Despite the differences in the numbers of neutrophils in the early phase, the absence of NKT cells did not appear to affect the number of neutrophils or macrophages at 96 hours. As shown in Figure 4B, histologic examination revealed that B6 mice and Jα18KO mice (same as CD1d KO mice; data not shown) had equivalent levels of damage to the anterior segment of the eye.

In addition to numbers of neutrophils and macrophages, we also determined the ratio of T lymphocytes in the corneal infiltrating cell at 96 hours. As shown in Figure 4C, the ratio of TCR^+ T lymphocytes was approximately 1% of total infiltrating cells. We thus speculated that conventional T cells play a minimum role in this model.

NKT Cell-Dependent Suppression Was Not Caused by VEGF-Mediated Vascularization

We compared the lengths and areas of corneal neovascularization in control mice and NKT-deficient mice and found no significant differences at 24 or 96 hours after cauterization (Fig. 5). However, the cauterized corneas of the NKT cell-deficient mice expressed high levels of VEGF at 24 hours (Fig. 2). To determine whether the increased inflammation at 96 hours was initiated by a VEGF-associated vascularization process, we compared the angiogenic ability in response to VEGF between both types of NKT cell-deficient mice and control mice. As shown in Figure 6, there was no significant difference in the ability to form new vessels, suggesting that NKT cells can regulate corneal inflammation (edema and opacity) but not VEGF-mediated corneal angiogenesis.

NKT Cells Accumulated to the Cornea in the Early Phase

To investigate the mechanism of NKT-dependent early neutrophil accumulation, we used RT-PCR to determine the location of NKT cells. We hypothesized that NKT cells would localize to the cornea during the early phase, where they would produce specific chemokines to recruit neutrophils. However, in con-

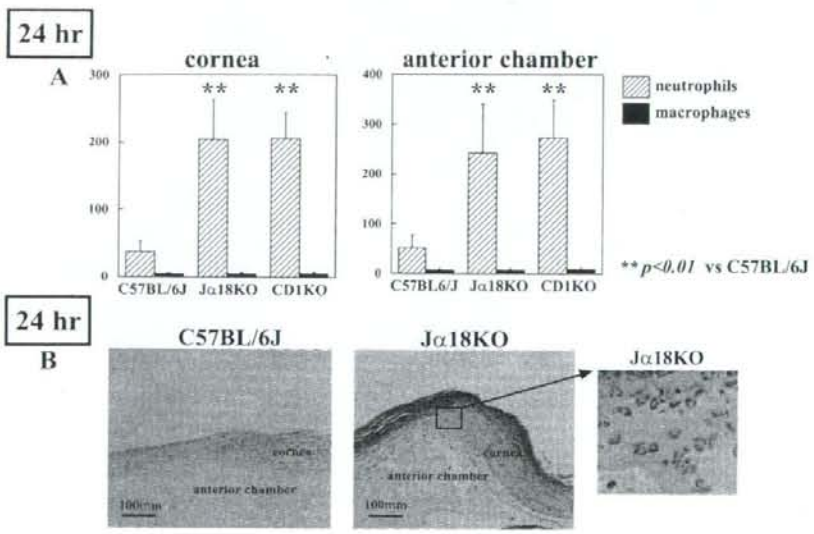

FIGURE 3. Corneal inflammation in NKT-deficient mice. Right eyes (n = 5) were removed at 24 hours after cauterization. Sections (4 μm) were stained with hematoxylin and eosin, numbers of neutrophils and macrophages were counted in three independent visual fields (magnification, ×200) in the cornea and anterior chamber, and the averages were calculated. (**A**) Early infiltration of neutrophils (*solid black bars*) and macrophages (*hatched bars*) in control (B6; n = 10), Jα18-KO (n = 10), and CD1d-KO (n = 10) mice. The experiment was performed twice with similar results. (**B**) Histologic sections of cauterized corneas from control (B6) and Jα18-KO mice, with an enlarged area of the Jα18-KO sample shown on the *right*.

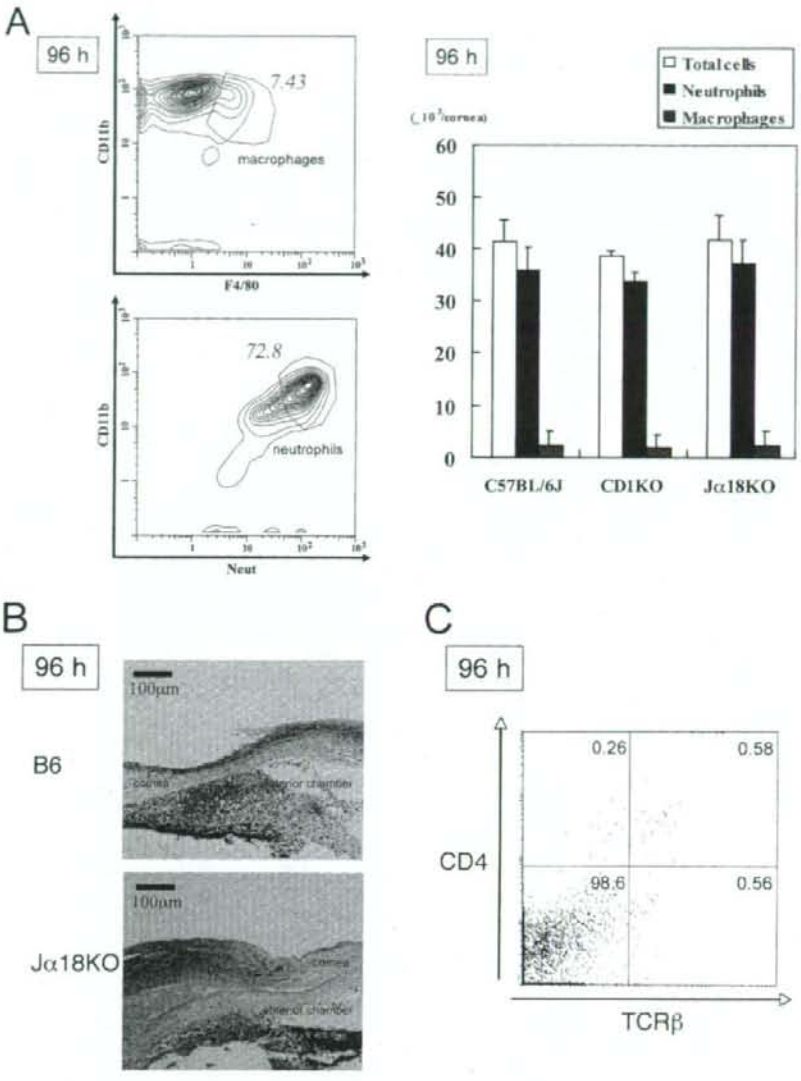

FIGURE 4. Corneal-infiltrating neutrophils and macrophages after cauterization. Inflammatory cells were isolated from corneas 96 hours after cauterization. Three corneas were pooled to obtain enough viable cells for flow cytometry. Eighteen corneas were examined as six pooled samples of three individual eyes. (**A**, *left*) Typical discriminative plots of corneal-infiltrating neutrophils (7/4) and macrophages (F4/80) by flow cytometry in control C57BL/6 mice. *Right*: analysis of corneal cell infiltrates in control (C57BL/6J) and NKT cell-deficient (CD1 KO and Jα18 KO) mice. The experiment was performed three times with similar results. No significant differences were detected. (**B**) Histologic sections of cauterized corneas from control (B6) and Jα18-KO (96 hours) mice. (**C**) Analysis of TCR^+ cells in cornea (96 hours).

trast to our hypothesis, we could not detect Vα14 gene expression in the inflamed corneas until 96 hours after cauterization (Fig. 7A).

As shown in Figure 4C, the number of corneal infiltrating TCR^+ cells was extremely low, so we knew there was a possibility we could not detect changes by conventional RT-PCR. In addition, it has reported that CXCR6 is another marker for NKT cells (the ligand is CXCL16).[34] We thus attempted to detect the difference in the expression of the *Vα14* and *CXCR6* genes in the cauterized cornea in the early phase by quantitative real-time PCR. As shown in Figure 7B, we observed a significant increase in the expression of the *Vα14* and *CXCR6* genes in the cauterized cornea (24 hours). Compared with the positive control (spleen), the expression levels of *Vα14* and *CXCR6* were extremely low, and the difference could not be detected by conventional RT-PCR. However, we detected significant differences with quantitative real-time PCR.

DISCUSSION

NKT cells promote systemic tolerance associated with the eye and ACAID[29] and are required for the generation of allospecific regulatory T cells after orthotropic corneal transplantation. It is important to distinguish the nonspecific acute corneal inflammation that occurs after injuries from corneal graft rejection. The former is mediated by macrophages and neutrophils,[7,8] whereas the latter are mediated by allospecific T cells.[27] We therefore focused on the role of NKT cells in acute corneal inflammation after cauterization in the present study.

Our data indicate that CD1d-restricted NKT cells play an important role in the formation of acute nonspecific corneal inflammation induced by exogenous, dangerous stimuli, such as cauterization. Independent NKT cell-deficient (CD1d-KO and Jα18-KO) mice demonstrated accelerated corneal inflammation and enhanced early (24-hour) corneal accumulation of

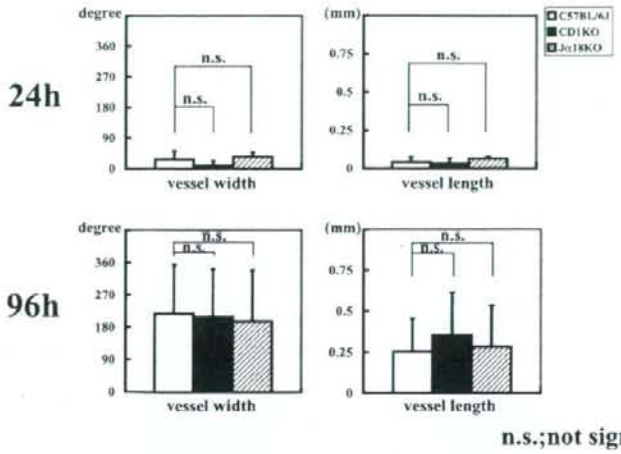

FIGURE 5. Evaluation of new corneal vessels after cauterization. Cauterized corneas ($n = 5$) from control (C57BL/6J) and NKT cell-deficient (CD1 KO and Jα18 KO) mice were evaluated for corneal neovascularization, by length and extension, 24 and 96 hours after cauterization. The experiment was performed twice with similar results. No significant differences were detected.

neutrophils. Both strains of mice also upregulated VEGF, TNFα, and IFNγ in the cornea 24 hours after cauterization. Thus, we concluded that NKT cells regulate the early accumulation of neutrophils and protect the cornea from excessive inflammation.

The increase in the number of neutrophils was temporary and was observed at 24 hours but not at 96 hours after cauterization. We postulate that early-accumulated neutrophils must be important for initiating functional changes and for activating infiltrating macrophages and corneal resident cells (such as keratocytes) critical for the further development of corneal inflammation.[34,35] This might explain why both types of NKT cell-deficient mice showed severe corneal edema and opacity 96 hours later, even though the number of neutrophils and macrophages was not significantly reduced at this time.

Our data contrast with the finding that NKT cells promote neutrophil accumulation in a lipopolysaccharide-induced hepatitis model[36] and in corneal *Pseudomonas aeruginosa* infection.[37] These studies also showed that NKT cell-deficient mice had reduced areas of hepatic injury and corneal IFNγ production. The reason for this discrepancy in our own results is unclear. However, NKT cells have the multipotential to regulate the immune response, and the type of reaction in vivo varies according to the systems or organs. Indeed, in vivo treatment of αGalCer, which is an NKT cell ligand, induced the production of either T-helper 1 (Th1) or Th2 cytokines, depending on the dose and timing of the inoculations.[38] The environmental differences between the eye and the liver may be reflected by the type of NKT cell activation.

Although corneal angiogenesis is an important step in the development of corneal edema and opacity, the two processes could be separate. Our study focused on corneal edema and opacity, which are directly associated with loss of visual acuity in patients, rather than on corneal angiogenesis. Even though both types of NKT cell-deficient mice expressed higher levels of VEGF in the cornea, early VEGF expression did not augment corneal neovascularization in these animals (Fig. 5), which we confirmed with the corneal micropocket assay embedded with exogenous VEGF (Fig. 6). The difference in corneal inflammation between wild-type mice and NKT cell-deficient mice was not dependent on the growth of new corneal vessels induced by VEGF. However, it is known that VEGF is not merely an angiogenic factor but that it is also a proinflammatory cytokine.[39] Early VEGF can, therefore, still affect the subsequent inflammatory process in the cauterized cornea.

Although the number of recruited NKT cells must have been very small (Fig. 4B), we could detect significant differences in the expression of the *Vα14* and *CXCR6* genes with the use of quantitative real-time PCR. NKT cells can be effective, even in low numbers, in initiating immune reactions.[9,10] NKT cells might regulate neutrophil function in their natural state or development level. Indeed, Hwang et al.[40] previously

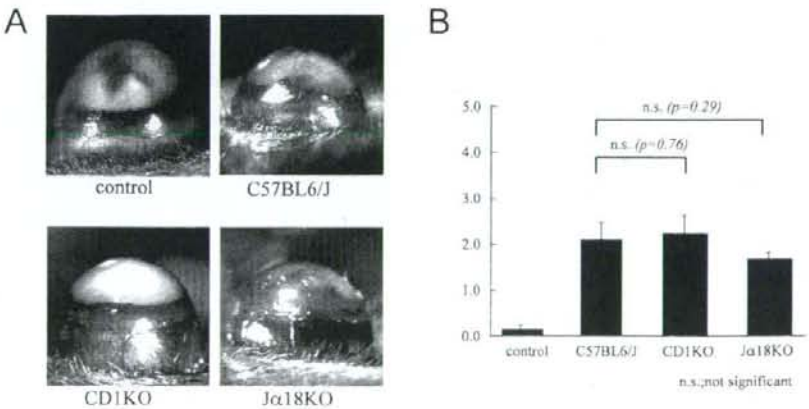

FIGURE 6. Comparison of new vessel-forming ability against exogenous VEGF expression. (**A**) Poly(hydroxyethyl) methacrylate pellet-embedded corneas of control (C57BL/6J) and NKT cell-deficient (CD1 KO and Jα18 KO) mice after 96 hours on corneal micropocket assay. (**B**) Evaluation of corneal neovascularization induced by exogenous VEGF showed no significant difference between control (C57BL/6J) and NKT cell-deficient (CD1 KO and Jα18 KO) mice. The experiment was performed twice with similar results.

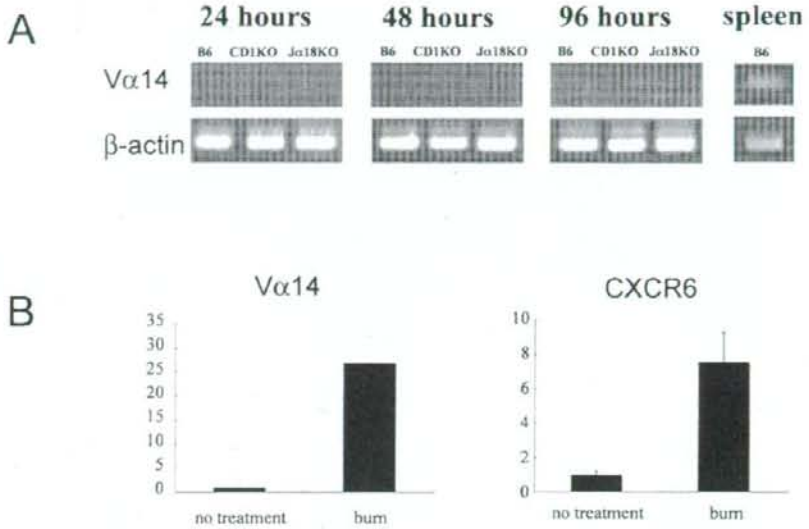

FIGURE 7. *Vα14* gene expression in cauterized corneas. (**A**) The right eyes ($n = 3$) were removed at 24, 48, and 96 hours after cauterization from control (B6) and NKT cell-deficient (CD1 KO and Jα18 KO) mice, and total corneal mRNA was extracted for the examination of *Vα14* mRNA. Three corneas were pooled to obtain sufficient mRNA. The experiment was performed twice with similar results. (**B**) Nontreated ($n = 3$) and cauterized ($n = 3$) corneas at 24 hours were removed, and levels of *Vα14* and *CXCR6* mRNA were examined by quantitative real-time PCR. The experiment was performed twice with similar results.

demonstrated the hyperactivity of neutrophils in NKT-deficient mice, which could be the reason for early neutrophil accumulation after corneal cauterization.

Our data indicate a protective role for CD1d-restricted invariant NKT cells against nonspecific corneal inflammation. In vivo stimulation of NKT cells by their specific ligands may have potential for use in therapeutic intervention. Further study is required to elucidate the role of NKT cells in various corneal disorders associated with inflammation.

Acknowledgments

The authors thank Mari Imamura and Michiyo Takahara for their excellent technical support.

References

1. Streilein JW. Ocular immune privilege: therapeutic opportunities from an experiment of nature. *Nat Rev Immunol.* 2003;3:879–889.
2. Griffith TS, Brunner T, Fletcher SM, Green DR, Ferguson TA. Fas ligand-induced apoptosis as a mechanism of immune privilege. *Science.* 1995;270:1189–1192.
3. Taylor AW, Streilein JW, Cousins SW. Identification of alpha-melanocyte stimulating hormone as a potential immunosuppressive factor in aqueous humor. *Curr Eye Res.* 1992;11:1199–1206.
4. Taylor AW, Streilein JW, Cousins SW. Immunoreactive vasoactive intestinal peptide contributes to the immunosuppressive activity of normal aqueous humor. *J Immunol.* 1994;153:1080–1086.
5. Hazlett LD. Role of innate and adaptive immunity in the pathogenesis of keratitis. *Ocul Immunol Inflamm.* 2005;13:133–138.
6. Dana MR. Angiogenesis and lymphangiogenesis: implications for corneal immunity. *Semin Ophthalmol.* 2006;21:19–22.
7. Sonoda KH, Nakao S, Nakamura T, et al. Cellular events in the normal and inflamed cornea. *Cornea.* 2005;24:S50–S54.
8. Oshima T, Sonoda KH, Tsutsumi-Miyahara C, et al. Analysis of corneal inflammation induced by cauterisation in CCR2 and MCP-1 knockout mice. *Br J Ophthalmol.* 2006;90:218–222.
9. Bendelac A, Rivera MN, Park SH, Roark JH. Mouse CD1-specific NK1 T cells: development, specificity, and function. *Annu Rev Immunol.* 1997;15:535–562.
10. Taniguchi M, Harada M, Kojo S, Nakayama T, Wakao H. The regulatory role of Valpha14 NKT cells in innate and acquired immune response. *Annu Rev Immunol.* 2003;21:483–513.
11. Lantz O, Bendelac A. An invariant T cell receptor alpha chain is used by a unique subset of major histocompatibility complex class I-specific $CD4^+$ and $CD4^-8^-$ T cells in mice and humans. *J Exp Med.* 1994;180:1097–1106.
12. Makino Y, Kanno R, Ito T, Higashino K, Taniguchi M. Predominant expression of invariant V alpha 14+ TCR alpha chain in NK1.1+ T cell populations. *Int Immunol.* 1995;7:1157–1161.
13. Porcelli S, Yockey CE, Brenner MB, Balk SP. Analysis of T cell antigen receptor (TCR) expression by human peripheral blood $CD4^-8^-$ α/β T cells demonstrates preferential use of several V beta genes and an invariant TCR alpha chain. *J Exp Med.* 1993;178:1–16.
14. Bendelac A, Lantz O, Quimby ME, Yewdell JW, Bennink JR, Brutkiewicz RR. CD1 recognition by mouse NK1+ T lymphocytes. *Science.* 1995;268:863–865.
15. Exley M, Garcia J, Balk SP, Porcelli S. Requirements for CD1d recognition by human invariant $Va24^+$ $CD4^-$ $CD8^-$ T cells. *J Exp Med.* 1997;186:109–120.
16. Chen YH, Chiu NM, Mandal M, Wang N, Wang CR. Impaired NK1+ T cell development and early IL-4 production in CD1-deficient mice. *Immunity.* 1997;6:459–467.
17. Mendiratta SK, Martin WD, Hong S, Boesteanu A, Joyce S, Van Kaer L. CD1d1 mutant mice are deficient in natural T cells that promptly produce IL-4. *Immunity.* 1997;6:469–477.
18. Smiley ST, Kaplan MH, Grusby MJ. Immunoglobulin E production in the absence of interleukin-4-secreting CD1-dependent cells. *Science.* 1997;275:977–979.
19. Cui J, Shin T, Kawano T, et al. Requirement for Vα14 NKT cells in IL-12-mediated rejection of tumors. *Science.* 1997;278:1623–1626.
20. Ito K, Karasawa M, Kawano T, et al. Involvement of decidual Vα14 NKT cells in abortion. *Proc Natl Acad Sci USA.* 2000;97:740–744.
21. Matsuzaki G, Li XY, Kadena T, et al. Early appearance of T cell receptor alpha beta + $CD4^-$ $CD8^-$ T cells with a skewed variable region repertoire after infection with *Listeria monocytogenes*. *Eur J Immunol.* 1995;25:1985–1991.
22. Apostolou I, Takahama Y, Belmant C, et al. Murine natural killer T(NKT) cells [correction of natural killer cells] contribute to the granulomatous reaction caused by mycobacterial cell walls. *Proc Natl Acad Sci USA.* 1999;96:5141–5146.
23. Sumida T, Sakamoto A, Murata H, et al. Selective reduction of T cells bearing invariant V alpha 24J alpha Q antigen receptor in patients with systemic sclerosis. *J Exp Med.* 1995;182:1163–1168.
24. Baxter AG, Kinder SJ, Hammond KJ, Scollay R, Godfrey DI. Association between $\alpha\beta$TCR$^+$ $CD4^-$ $CD8^-$ T-cell deficiency and IDDM in NOD/Lt mice. *Diabetes.* 1997;46:572–582.

25. Seino KI, Fukao K, Muramoto K, et al. Requirement for natural killer T (NKT) cells in the induction of allograft tolerance. *Proc Natl Acad Sci USA*. 2001;98:2577–2581.
26. Iwai T, Tomita Y, Okano S, et al. Regulatory roles of NKT cells in the induction and maintenance of cyclophosphamide-induced tolerance. *J Immunol*. 2006;177:8400–8409.
27. Sonoda Y, Streilein JW. Impaired cell-mediated immunity in mice bearing healthy orthotopic corneal allografts. *J Immunol*. 1993; 150:1727–1734.
28. Sonoda KH, Taniguchi M, Stein-Streilein J. Long-term survival of corneal allografts is dependent on intact CD1d-reactive NKT cells. *J Immunol*. 2002;168:2028–2034.
29. Sonoda KH, Exley M, Snapper S, Balk SP, Stein-Streilein J. CD1-reactive natural killer T cells are required for development of systemic tolerance through an immune-privileged site [see comments]. *J Exp Med*. 1999;190:1215–1226.
30. Sonoda K, Sakamoto T, Yoshikawa H, et al. Inhibition of corneal inflammation by the topical use of Ras farnesyltransferase inhibitors: selective inhibition of macrophage localization. *Invest Ophthalmol Vis Sci*. 1998;39:2245–2251.
31. Seo SK, Gebhardt BM, Lim HY, et al. Murine keratocytes function as antigen-presenting cells. *Eur J Immunol*. 2001;31:3318–3328.
32. Kuwano T, Nakao S, Yamamoto H, et al. Cyclooxygenase 2 is a key enzyme for inflammatory cytokine-induced angiogenesis. *FASEB J*. 2004;18:300–310.
33. Nakao S, Kuwano T, Tsutsumi-Miyahara C, et al. Infiltration of COX-2-expressing macrophages is a prerequisite for IL-1 beta-induced neovascularization and tumor growth. *J Clin Invest*. 2005; 115:2979–2991.
34. Jiang X, Shimaoka T, Kojo S, et al. Critical role of CXCL16/CXCR6 in NKT cell trafficking in allograft tolerance. *J Immunol*. 2005; 175:2051–2055.
35. Oakes JE, Monteiro CA, Cubitt CL, Lausch RN. Induction of interleukin-8 gene expression is associated with herpes simplex virus infection of human corneal keratocytes but not human corneal epithelial cells. *J Virol*. 1993;67:4777–4784.
36. Diao H, Kon S, Iwabuchi K, et al. Osteopontin as a mediator of NKT cell function in T cell-mediated liver diseases. *Immunity*. 2004;21:539–550.
37. Hazlett LD, Li Q, Liu J, et al. NKT cells are critical to initiate an inflammatory response after *Pseudomonas aeruginosa* ocular infection in susceptible mice. *J Immunol*. 2007;179:1138–1146.
38. Bendelac A, Savage PB, Teyton L. The biology of NKT cells. *Annu Rev Immunol*. 2006;25:297–336.
39. Lee YC. The involvement of VEGF in endothelial permeability: a target for anti-inflammatory therapy. *Curr Opin Investig Drugs*. 2005;6:1124–1130.
40. Hwang SJ, Kim S, Park WS, Chung DH. IL-4-secreting NKT cells prevent hypersensitivity pneumonitis by suppressing IFN-gamma-producing neutrophils. *J Immunol*. 2006;177:5258–5268.

THE JOURNAL OF GENE MEDICINE
J Gene Med 2008; **10**: 165–176.
Published online 12 December 2007 in Wiley InterScience (www.interscience.wiley.com) **DOI:** 10.1002/jgm.1142

RESEARCH ARTICLE

Newly-developed Sendai virus vector for retinal gene transfer: reduction of innate immune response via deletion of all envelope-related genes

Yusuke Murakami,[1,2] Yasuhiro Ikeda,[2]* Yoshikazu Yonemitsu,[1,3] Sakura Tanaka,[1] Haruhiko Kondo,[1] Shinji Okano,[1] Ri-ichiro Kohno,[2] Masanori Miyazaki,[2] Makoto Inoue,[4] Mamoru Hasegawa,[4] Tatsuro Ishibashi,[2] Katsuo Sueishi,[1†]

[1]*Division of Pathophysiological and Experimental Pathology, Department of Pathology, Graduate School of Medical Sciences, Kyushu University, Fukuoka, Japan;* [2]*Department of Ophthalmology, Graduate School of Medical Sciences, Kyushu University, Fukuoka, Japan;* [3]*Department of Gene Therapy at the 21st Century COE program, Chiba University Graduate School of Medicine, Chiba, Japan;* [4]*DNAVEC Corporation, Tsukuba-city, Ibaraki, Japan*

*Correspondence to: Yasuhiro Ikeda, Department of Ophthalmology, Graduate School of Medical Sciences, Kyushu University, 3-1-1 Maidashi, Higashi-ku, Fukuoka, 812-8582, Japan. E-mail: ymocl@pathol1.med.kyushu-u.ac.jp

†Reprint requests to: Katsuo Sueishi, Division of Pathophysiological and Experimental Pathology, Department of Pathology, Graduate school of Medical Sciences, Kyushu University, 3-1-1 Maidashi, Higashi-ku, Fukuoka, 812–8582, Japan. E-mail address: sueishi@pathol1.med.kyushu-u.ac.jp.

Received: 5 July 2007
Revised: 7 October 2007
Accepted: 26 October 2007

Abstract

Background Recombinant Sendai virus vectors (rSeV) constitute a new class of cytoplasmic RNA vectors that have shown efficient gene transfer in various organs, including retinal tissue; however, the related immune responses remain to be overcome in view of clinical applications. We recently developed a novel rSeV from which all envelope-related genes were deleted (rSeV/dFdMdHN) and, in the present study, assess host immune responses following retinal gene transfer.

Methods rSeV/dFdMdHN or conventional F-gene deleted rSeV (rSeV/dF) was injected into subretinal space of adult Wistar rats or C57BL/6 mice. The transgene expression and histopathological findings were assessed at various time points. Immunological assessments, including the expression of proinflammatory cytokines, natural killer (NK)-cell activity, as well as SeV-specific cytotoxic T lymphocytes (CTLs) and antibodies, were performed following vector injection.

Results rSeV/dFdMdHN showed high gene transfer efficiency into the retinal pigment epithelium at an equivalent level to that seen with rSeV/dF. In the early phase, the upregulation of proinflammatory cytokines, local inflammatory cell infiltration and tissue damage that were all prominently seen in rSeV/dF injection were dramatically diminished using rSeV/dFdMdHN. NK cell activity was also decreased, indicating a reduction of the innate immune response. In the later phase, on the other hand, CTL activity and anti-SeV antibodies were similarly induced, even using rSeV/dFdMdHN, and resulted in transient transgene expression in both vector types.

Conclusions Deletion of envelope-related genes of rSeV dramatically reduces the vector-induced retinal damage and may extend the utility for ocular gene transfer; however, further studies regulating the acquired immune response are required to achieve long-term transgene expression of rSeV. Copyright © 2007 John Wiley & Sons, Ltd.

Keywords envelope-related genes; innate immune response; recombinant Sendai virus; retinal gene therapy

Introduction

Clinical trials of gene therapy as a new treatment strategy for ocular diseases, such as age-related macular degeneration or retinoblastoma, have demonstrated encouraging results [1,2]. One advantage of the eyes for gene therapy is the anatomical fact of their being relatively small and isolated organs, which enables efficient gene transfer with a limited number of virus vectors and limited systemic exposure [3].

Several vector systems are now available and have made further modifications for successful gene therapy; however, much investigation remains to be done to establish its efficacy and safety.

Sendai virus (SeV) is an enveloped virus with a non-segmented negative-strand RNA genome and is a member of the family *Paramyxoviridae*. It contains six major genes arranged in tandem on its genome: three virus-derived proteins [nucleoprotein (NP), phosphoprotein (P) and large protein (L)] form a ribonucleoprotein complex (RNP) with the SeV genomic RNA, and the RNP acts as a template for transcription and replication. The other three envelope-related proteins [haemagglutinin-neuraminidase (HN), fusion protein (F) and matrix protein (M)] mediate the attachment of virions, penetration of RNPs into infected cells, and virion formation, respectively [4].

SeV makes use of sialic acid residue on surface glycoproteins or asialoglycoprotein present as a receptor [5,6], and SeV-derived vectors (recombinant SeV: rSeV) have been shown to infect various types of mammalian cells, such as airway epithelial, skeletal muscle, ependymal and vascular endothelial cells, and produce two- to three-fold log higher gene transfer efficiency than adenoviral vectors or lipofection [7,8]. The gene transfer and expression take place in the cytoplasm without a DNA phase in the life cycle [9], avoiding possible malignant transformation due to genetic alteration of host cells, which is a safety advantage of rSeV. For use in human gene therapy, we have constructed F-deficient rSeVs (rSeV/dF), which show non-self-transmissible properties, as the first generation of clinically available rSeVs [10]. This type of rSeV still produces efficient gene transfer, and has been employed since 1 February 2006 in an ongoing clinical study of therapeutic angiogenesis for the treatment of critical limb ischemia at Kyushu University after approval by Institutional and Governmental Review Boards.

In ocular tissue, transmissible-type rSeVs exhibited efficient gene transfer to the retinal pigment epithelium (RPE) of the rat retina via subretinal injection; however, the gene expression was markedly decreased 7 days after injection [11]. The transgene expression was prolonged by immunosuppressants, such as corticosteroids or cyclosporine A, suggesting that host immune responses play an important role in eliminating viruses. Despite some advantageous features of rSeV in clinical gene therapy strategies, the related immune responses against SeV and the consequential tissue damage have been too hazardous to expand its utility in some clinical settings, especially for neurosensory tissues such as the retina. Host immune responses remain almost unchanged with the use of rSeV/dF (unpublished data), suggesting that the first generation is still not applicable for retinal gene therapy.

To enhance the safety and efficacy of this procedure, we recently developed a new rSeV vector that is deficient in all the membranous genes (rSeV/dFdMdHN), and succeeded in recovering this vector at high titers. This vector has shown transduction efficacy equal to that of rSeV/dF, and reduced cytototoxicity *in vitro* and *in vivo* [12]. Furthermore, we recently found that rSeV/dFdMdHN significantly reduces host immune responses in pulmonary gene transfer [13]. These vector-related immune responses might be further reduced in retinal gene transfer because the eye is known as an immune privileged site [14,15]. To obtain preclinical information regarding this new generation of rSeV in retinal tissue, in the present study, we assessed the *in vivo* gene transfer efficiency of rSeV/dFdMdHN into rat and mouse retinas and the effect on host immune responses in the early and late phases following vector injection.

Materials and methods

Recombinant Sendai virus vector

F, M and HN gene-deleted SeV vectors (rSeV/dFdMdHN) and F gene-deleted SeV vectors (rSeV/dF) were constructed as previously described [10,12]. The enhanced green fluorescent protein (EGFP) or firefly luciferase gene was inserted between the P and L genes of rSeV/dFdMdHN, and upstream of the NP gene of rSeV/dF. The schematic genome structures of SeV vectors are shown in supplementary Figure 1. The titers of recovered viral vectors were expressed as cell infectious units (ciu) [10]. We repeatedly confirmed the vector titers, and the final products were also highly purified via chromatography.

Animals

Six-week-old male Wistar rats and 8-week-old female C57BL/6 mice were maintained humanely, with proper institutional approval, and in accordance with the ARVO Statement for the Use of Animals in Ophthalmic and Vision Research. All animal experiments were carried out under approved protocols and in accordance with the recommendations for the proper care and use of laboratory animals by the Committee for Animals, Recombinant DNA, and Infectious Pathogens Experiments at Kyushu University and according to The Law (No.105) and Notification (No.6) of the Japanese Government.

Gene transfer procedures

The subretinal injection of each solution was performed as previously described with minor modifications [11,16]. Briefly, rats or mice were anaesthetized by inhalation ether. The following procedures were then performed using an operating microscope. A 30-gauge needle was inserted into the subretinal space of the peripheral retina in the nasal hemisphere via an external transscleral transchoroidal approach. The vector solution (10 μl)

(rSeV/dFdMdHN or rSeV/dF) or BSS: (137 mM NaCl, 5.3 mM KCl, 0.44 mM KH_2PO_4, 0.34 mM Na_2HPO_4 and 13 mM Tris, pH7.6) was injected, and excess solution from the injection site was washed out using phosphate-buffered saline (PBS). Approximately 3 µl of solution remained in the subretinal space (data not shown). The appearance of a dome-shaped retinal detachment confirmed the subretinal delivery. Eyes that sustained prominent surgical trauma, such as retinal or subretinal haemorrhage or bacterial infection, were excluded from this examination.

Detection and examination of GFP expression using fundus camera

Ophthalmoscopy was performed at various time points after gene transfer (days 2, 4, 7, 10 and 14) as previously described [17]. To detect GFP in the rat retina, we used a fundus camera (TRC-50X; Topcon, Tokyo, Japan), which is widely available as a clinical tool for fluorescein angiography.

Luciferase assay

Enucleated eyes were minced in 500 µl of 1× lysis buffer with a protease inhibitor cocktail, and centrifuged, after which 20 µl of the supernatants were subjected to luciferase assay as previously described [11,18]. Light intensity was measured by a luminometer (Model LB9507, EG&G Berthold, Bad Wildbad, Germany) with 10-s integration. The data are expressed as %RLU (relative light unit) standardized by the mean value of each RLU on day 2 following vector injection.

Histological examination

At each time point after gene transfer (days 2, 7 and 14), the eyes of animals injected with rSeV/dFdMdHN, rSeV/dF or BSS were enucleated, and both paraffin and cryosections were prepared. For paraffin sections, the eyes were fixed with ice-cooled 4% paraformaldehyde in PBS for 1 day at room temperature, and then mounted in paraffin. For cryosections, the eyes were frozen in liquid nitrogen. 5 µm-thick paraffin and cryosections were stained with haematoxylin and eosin, and examined under light microscopy.

Immunohistochemistry

Immunoperoxidase

Infiltrating inflammatory cells in the rat retina were identified by immunohistochemistry. The frozen sections were incubated overnight at 4 °C with primary antibodies: anti-rat CD68 monoclonal antibody (1 : 150, Mouse IgG1, Chemicon, Temecula, CA, USA) for monocytes/macrophages, and anti-rat CD45 monoclonal antibody (1 : 150, Mouse IgG1, Acris GmbH, Hidenhausen, Germany) for leukocytes. Then signals were developed using the avidin-biotinylated peroxidase complex method. For negative controls, the primary antibody was omitted.

Immunofluorescence

The localization of GFP expression was identified by immunofluorescence technique. Deparaffinized sections were incubated overnight at 4 °C with anti-GFP polyclonal antibody (1 : 300, Rabbit IgG, Molecular Probes, Eugene, OR, USA). Anti-rabbit IgG-FITC (1 : 50, Bovine, Santa Cruz, CA, USA) was used as a secondary antibody. All sections were counterstained with DAPI and mounted in Crystal/Mount. Immunofluorescence images were acquired using an Olympus BX51 microscope with a fluorescent attachment (Olympus Corp., Tokyo, Japan). For negative controls, the primary antibody was omitted.

Enzyme-linked immunosorbent assay (ELISA)

The amounts of interleukin (IL)-1β, IL-6, IL-10, interferon (IFN)-γ and tumor necrosis factor (TNF)-α in ocular tissue and serum were determined by ELISA. Commercially available assay systems were used (R&D Systems, Minneapolis, MN, USA). For ocular tissue preparation, conjunctival and muscular tissues were removed from enucleated eyes. The eyes were washed with PBS, minced with scissors in 500 µl of 1× lysis buffer with a protease inhibitor cocktail, and centrifuged at 15 000 r.p.m. for 5 min at 4 °C. The supernatants were subjected to ELISA according to the manufacturer's instructions.

^{51}Cr release assay for cytolytic activity of natural killer (NK) cells and cytotoxic T lymphocytes (CTLs)

Spleen cells were harvested from Wistar rats or C57BL/6 mice on day 2 after rSeV injection for NK cell-lysis assay, and from C57BL/6 mice on day 10 for CTL assay, and contaminated erythrocytes were depleted by 0.83% ammonium chloride. For NK cell-lysis assay, the splenocytes were directly used as NK effector cells. For CTL assay, 4×10^6 splenocytes were cultured with 1 µM SeV-peptide (Sigma, St Louis, MO, USA; H-2^b-restricted peptide) in 1 ml of complete medium in a 24-well culture plate. Two days later, 30 IU/ml human rIL-2 was added to the medium. After 5 days, the cultured cells were collected and used as CTL effector cells. Target cells [YAC-1, SeV-peptide pulsed EL-4, LCMV peptide (H-2^b-restricted peptide) pulsed EL-4 (for third party)] were labelled with 100 µCi $Na_2{}^{51}CrO_4$ for 1.5 h, and were cultured with the spleen cells at various effector-to-target cell ratios. After 4 h of incubation, radioactivities in the culture supernatants were counted with an automatic γ-counter. The percentage of specific ^{51}Cr release of triplicates was calculated as: [(experimental cpm –

spontaneous cpm)/(maximum cpm − spontaneous cpm)] ×100. Spontaneous release was always <10% of maximal Cr release (target cells in 1% Triton X-100).

Anti-SeV antibody

Anti-SeV antibodies in rat serum on day 30 after gene transfer were evaluated by ELISA kit (Wakamoto Pharmaceutical Co., Tokyo, Japan). Serum samples were used for ELISA after appropriate dilutions.

In vitro cytotoxic assay with rSeVs

ARPE-19 cells were seeded in 96-well plates at 3000 cells/well in serum-free Dulbecco's modified Eagle's medium-F12 and, 12 h later, either rSeV/dF or rSeV/dFdMdHN was added to each well at indicated concentrations. Forty-eight hours later, cell viability was assessed by a modified MTT assay using Cell Counting Kit-8 (Dojindo Laboratories, Kumamoto, Japan). Results were calculated as percentage viability standardized by the mean value of control group without rSeV.

TUNEL staining

TUNEL and quantification of TUNEL-positive cells were performed using Apoptosis Detection TACS TdT Kit (R&D Systems) according to the manufacturer's instructions. PE-conjugated streptavidin (1 : 50, BD Biosciences) was used as a secondary antibody. The number of TUNEL-positive cells in the ARPE-19 cells was counted in a masked fashion.

Statistical analysis

All values were expressed as the mean ± SEM. Data were analysed by one-way analysis of variance with Fisher's adjustment. $p < 0.05$ was considered statistically significant.

Results

Transduction efficiency of F, M and HN gene-deleted recombinant SeV

To assess the transduction efficiency, we first injected three different titers (2.5×10^6, 2.5×10^7, 2.5×10^8 ciu/ml) of rSeV/dFdMdHN expressing the EGFP (rSeV/dFdMdHN-EGFP) into the subretinal space of rats, and recorded GFP expression using a fundus camera 48 h after injection. The extent of GFP fluorescence corresponded with the vector-injected area in the middle (2.5×10^7 ciu/ml) and high (2.5×10^8 ciu/ml) titer groups; the expression level was dose-dependent (Figure 1a). Moreover, the GFP expression by rSeV/dFdMdHN was approximately equal to that by rSeV/dF with the same titer (Figures 1a and 1b). A histological assessment demonstrated that the transgene expression was located in the RPE layer (Figure 1c) as previously described [11].

Next, we assessed the time course of transgene expression in vector-injected eyes, monitored by firefly luciferase expression. The data are expressed as %RLU standardized by the mean value of each RLU on day 2 following vector injection. As shown in Figures 2a and 2b, the luciferase expression in rSeV/dF-injected eyes rapidly decreased to approximately 50% by day 4 in each titer group, whereas that in rSeV/dFdMdHN-injected eyes was sustained at this time point ($p < 0.05$, $n = 6–7$ each). However, a decline did occur on day 7, and the luciferase expression by both rSeV vectors had almost disappeared on day 14. We also confirmed the transgene expression in the same eye by a fundus camera, using GFP as a reporter. As with the results of luciferase expression, the GFP expression by rSeV/dFdMdHN was sustained until day 4, then decreased, and disappeared by day 10 following vector injection; by contrast, that by rSeV/dF showed a more rapid decrease (Supplementary Figure 2).

These findings indicate that the deletion of all membranous genes of rSeV might contribute to the delayed vector clearance, but does not result in persistent transgene expression in the rat retina.

Histopathological comparison of retinal tissue treated with rSeVs

To determine whether rSeV/dFdMdHN reduced the immunogenicity in the rat retina, we conducted a histopathological examination of the vector-injected eyes. We injected a middle titer of rSeV/dFdMdHN-EGFP or rSeV/dF-EGFP into the subretinal space and examined the vector-injected site at various time points (days 2, 7 and 14). On day 2 following vector injection, only a slight mononuclear cell infiltrate was seen around the RPE layer in both vector types. On day 7, severe infiltrate of inflammatory cells was found around the RPE and choroid plexus, and the retinal structure was significantly destructed by day 14 in eyes treated with rSeV/dF; by contrast, the retinal inflammation and tissue damage were remarkably reduced with rSeV/dFdMdHN at each time point (Figure 3a). Immunohistochemical studies revealed that both CD68-positive macrophages and CD45-positive leukocytes decreased in number in eyes treated with rSeV/dFdMdHN (Figure 3b). Similar results were obtained in high-titer groups, although the extent of inflammatory cells was more severe in the high-titer groups (Figure 3c).

Moreover, the histopathogical findings of the retinal tissue showed a critical difference between rSeV/dFdMdHN and rSeV/dF. The RPE layer did not break down in the eye treated with rSeV/dFdMdHN, probably due to the reduction of inflammatory responses and vector-related

J Gene Med 2008; **10**: 165–176.
DOI: 10.1002/jgm

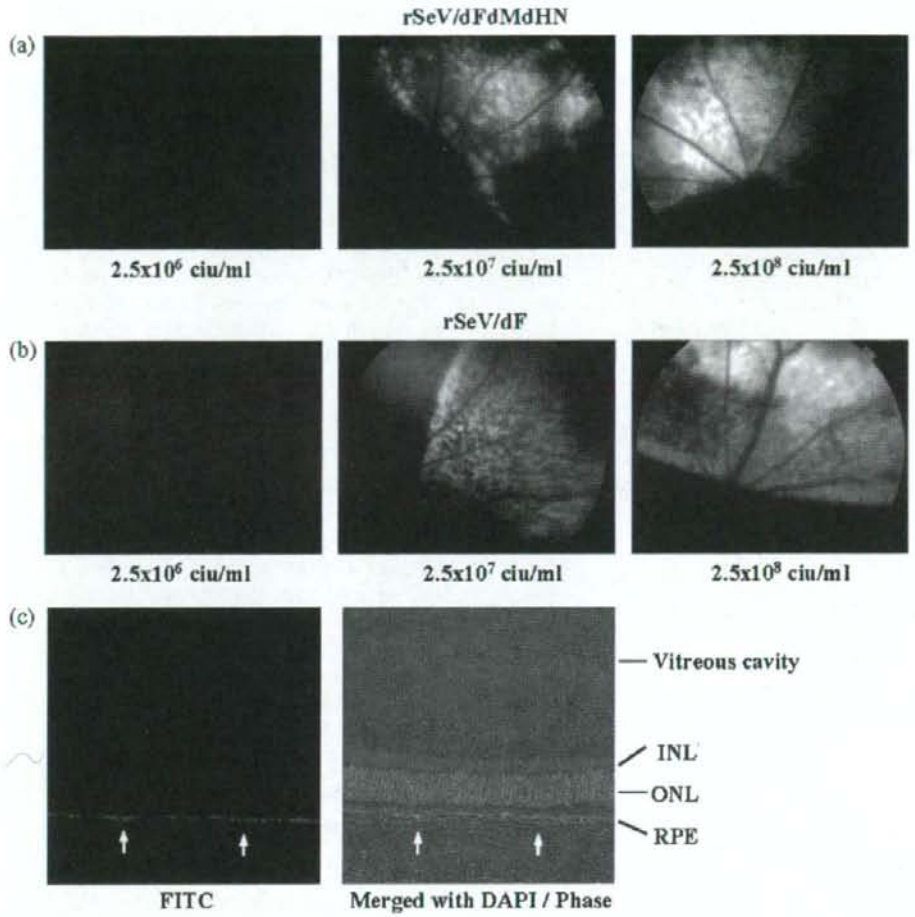

Figure 1. The GFP expression in the retinal fundus (a, b) and corresponding immunohistochemical findings (c) following subretinal injection of rSeV/dFdMdHN or rSeV/dF. (a, b) Three different titers (2.5×10^6, 2.5×10^7 and 2.5×10^8 ciu/ml) of rSeV/dFdMdHN-EGFP (a) or rSeV/dF-EGFP (b) were injected into the subretinal space of the rat retina, and the GFP expression was assessed by fundus camera on day 2 after injection. rSeV/dFdMdHN showed comparable GFP expression to rSeV/dF with the same titer. (c) The results of immunohistochemical studies against GFP on day 2 after rSeV/dFdMdHN-EGFP injection (2.5×10^8 ciu/ml). Note the strong staining in RPE (arrows), which was negative for control IgG antibodies (data not shown). INL, Inner nuclear layer; ONL, outer nuclear layer. Original magnification (c) ×200

cytotoxicity (Figures 3a and 3c). As a result, inflammatory cell infiltrate was not apparent over the RPE layer (in the neuroretina), and the structure of the retinal tissue was relatively preserved using rSeV/dFdMdHN (Figures 3a, 3b and 3c).

These findings clearly indicate a significant reduction of host immune responses and vector-induced retinal damage in retinal gene transfer by rSeV/dFdMdHN.

Reduced proinflammatory cytokine production and NK-cell cytotoxicity following gene transfer with rSeV/dFdMdHN

To determine the immune mechanisms underlying the histological differences between rSeV/dF and rSeV/dFdMdHN, we first evaluated the time course of expression of typical proinflammatory cytokines such as IL-1β, IL-6, TNF-α, IFN-γ and IL-10, which are known to be upregulated by respiratory infection with SeV [19]. ELISA revealed that the expressions of IL-1β and IFN-γ were immediately upregulated on day 2 following vector injection and sustained by day 7 in eyes that had been injected with rSeV/dF, whereas these cytokines were markedly reduced in rSeV/dFdMdHN-injected eyes in each titer group (Figures 4a and 4b, $p < 0.05$, $n = 5$–7each). Other cytokines (TNF-α, IL-6 and IL-10) were not detectable in the same samples (data not shown). In the serum, no significant increase of these inflammatory cytokines was seen during the time course (data not shown).

J Gene Med 2008; **10**: 165–176.
DOI: 10.1002/jgm

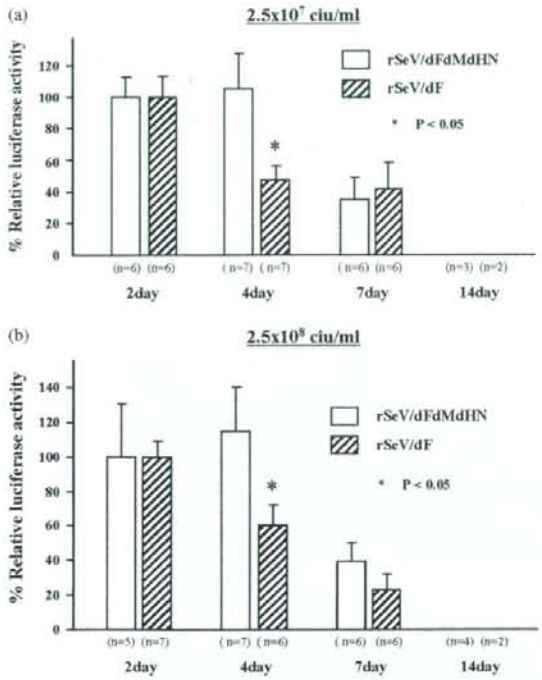

Figure 2. Time course of transgene expression mediated by each rSeV in rat retina. The eyes injected with a middle titer (2.5×10^7 ciu/ml) (a) or high titer (2.5×10^8 ciu/ml) (b) of each rSeV vector expressing firefly luciferase were subjected to luciferase assay. The data are expressed as %RLU (relative light unit) standardized by the mean value of each RLU on day 2 following vector injection. Note the delayed reduction of luciferase expression with rSeV/dFdMdHN (day 4, $n = 6–7$ each; $^*p < 0.05$)

Next, we evaluated NK cell activities, which are a crucial component of the innate immune response against virus infection [20,21]. Two days after vector injection or Poly I : C administration, the splenocytes were isolated and used for NK cell activity assay. Strong and significant upregulation of NK cell activity was observed in rats treated with high-titer rSeV/dF, as well as the positive controls (poly I:C), whereas no significant NK cell activity was found in rats treated with rSeV/dFdMdHN (Figure 5a). We also examined NK cell activities in C57BL/6 mice following subretinal injection of each rSeV vector, and found reduced NK cell activity in rSeV/dFdMdHN-treated mice (Figure 5b), as in the case of Wistar rats.

Together with data demonstrated in Figures 2–5, it has been suggested that, in eyes treated with rSeV/dF, expression of proinflammatory cytokines and NK cell activity are immediately increased within a few days, resulting in local infiltration of inflammatory cells and early vector clearance by days 4–7; by contrast, the deletion of membranous genes of rSeV remarkably attenuates these early responses, possibly contributing to the dramatic reduction of retinal inflammation and delay in vector clearance.

Assessment for adaptive immunity against rSeVs

To evaluate the late-phase immune response against rSeVs, we next examined both SeV-specific CTL activity and antibody production. For CTL assay, we used C57BL/6 strain mice (H-2^b), because the target amino acid residue of CTL against SeV has been identified as NP321–336 in this strain. Ten days after vector injection, the splenocytes were isolated, cultured with SeV-peptide and IL-2, and used for CTL assay. By contrast to NK cell cytotoxicity, CTLs from mice treated with rSeV/dFdMdHN showed strong cell lysis activity, which was higher than those from rSeV/dF-treated mice in each titer group (Figure 6a, left panel). As a control experiment, third-party peptide (lymphocytic choriomeningitis virus, LCMV) was used as a target, and no significant release was observed (Figure 6a, right panel).

Next, we evaluated the serum levels of anti-SeV antibody 4 weeks after each vector injection using ELISA. As shown in Figure 6b, no significant reduction in serum levels of anti-SeV antibody was found in both rats and mice treated with rSeV/dFdMdHN in each titer group ($n = 3–5$ each).

These findings suggest that the deletion of membranous genes of SeV have no significant effect on adaptive immune response, leading to the vector clearance by day 14 after injection as shown in Figure 2.

Reduced cytopathic effect of rSeV/dFdMdHN *in vitro*

Infection by rSeV causes some cytopathic effects and induces apoptosis in some types of cells [22]. As a final assessment, we examined the cytopathic effects of each rSeV on ARPE-19 cells, a human RPE-derived cell line. We cultured ARPE-19 cells in the presence of each rSeV and assessed the cellular viability after 48 h of culturing. A mild but significant reduction of cellular viability was found in cells with rSeV/dF in a dose-dependent manner, but not with rSeV/dFdMdHN (Figure 7a, $p < 0.01$, $n = 4$ each). Terminal dUTP-nicked end labelling (TUNEL) stain revealed that infection with rSeV/dF induced apoptosis in $10.9 \pm 1.3\%$ of ARPE-19 cells. By contrast, infection with rSeV/dFdMdHN almost completely suppressed the appearance of TUNEL-positive cells ($1.4 \pm 0.2\%$) (Figures 7b and 7c, $p < 0.01$, $n = 5$ each).

In addition to the effect on inflammatory responses, these data suggest that rSeV/dFdMdHN reduce the cytotoxicity and suppress the apoptosis of infected cells.

Discussion

In the present study we characterized *in vivo* retinal gene transfer using a new-generation Sendai virus vector

J Gene Med 2008; **10**: 165–176.
DOI: 10.1002/jgm

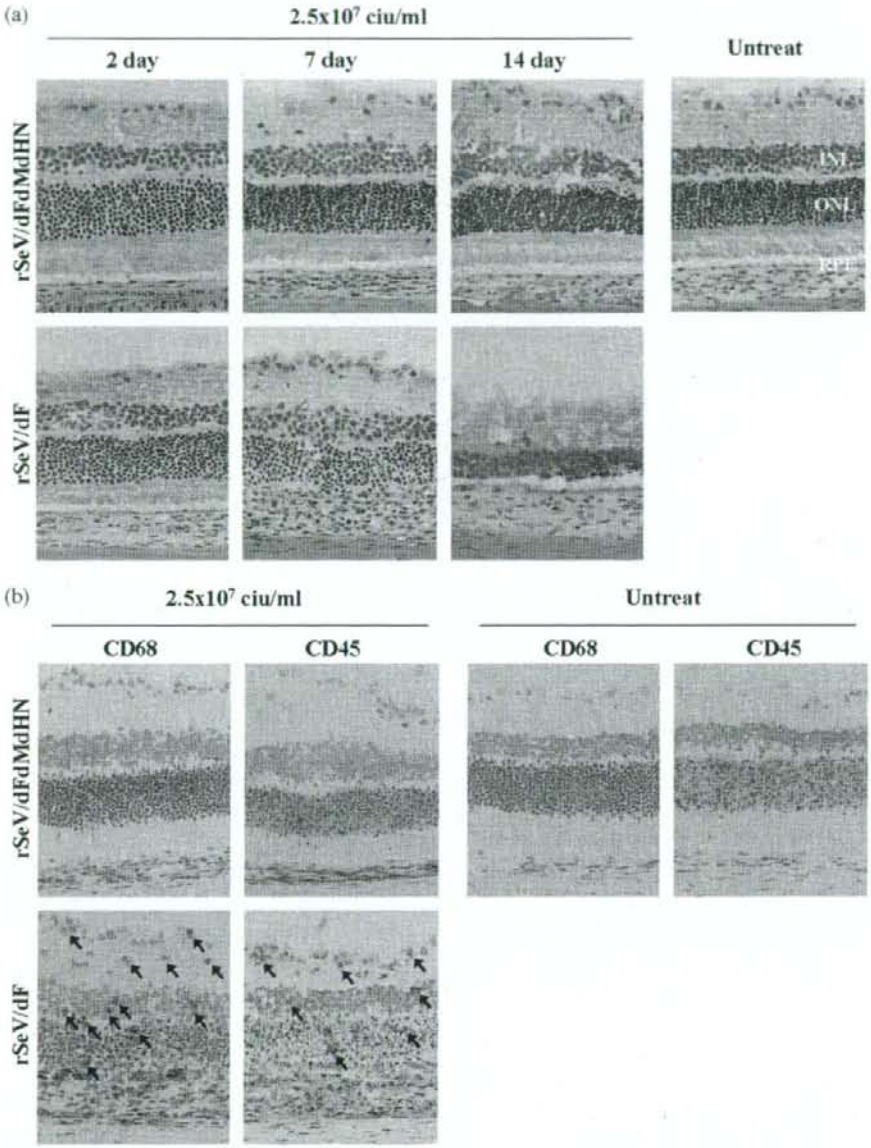

Figure 3. Histopathological (a, c) and immunohistochemical (b) findings of rat eyes injected with each rSeV. (a) Longitudinal sections of eyes injected with a middle titer (2.5×10^7 ciu/ml) of rSeV/dFdMdHN-EGFP or rSeV/dF-EGFP on days 2, 7 and 14 after gene transfer. The eyes treated with rSeV/dF showed severe inflammation around RPE and choroid plexus peaked on day 7 and tissue destruction on day 14. Note the marked reduction of inflammatory cell infiltrate in the rSeV/dFdMdHN-injected eyes. (b) Immunohistochemical findings in serial sections on day 7. Positive reaction (brown staining) of $CD68^+$ and $CD45^+$ cells are demonstrated. Note that some $CD68^+$ and $CD45^+$ cells infiltrate into the neuroretina in rSeV/dF-injected eyes (arrows) but not in rSeV/dFdMdHN-injected eyes. (c) Histopathological and immunohistochemical findings of rat retina injected with a high titer (2.5×10^8 ciu/ml) of rSeV vectors on day 7. Arrows indicate the infiltration of CD68+ and CD45+ cells into the neuroretina. Original magnifications (a, b, c) ×200

from which all membranous genes had been deleted, and compared the results with those using rSeV/dF, the presently available clinical vector. The major findings provided by our study were that: (i) subretinal injection of rSeV/dFdMdHN resulted in efficient transgene expression in RPEs, in a dose-dependent manner; (ii) a delay in vector clearance in the retina was observed approximately 4 days after gene transfer, but the transgene expression was diminished by day 14; (iii) histopathologically, the local infiltration of inflammatory cells was decreased, and the RPE layer and retinal structure were well preserved; (iv) both the early production of proinflammatory cytokines

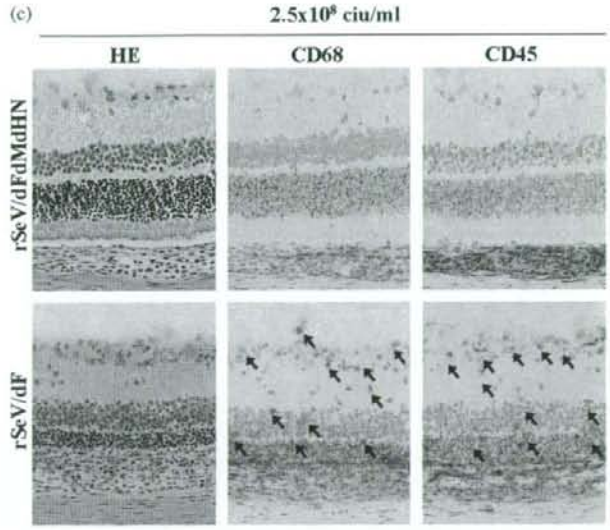

Figure 3. (*Continued*)

and NK cell cytotoxicity were significantly reduced, indicating a reduction of the innate immune response; and (v) significant levels of SeV-specific CTL and antibody were nevertheless induced. The most important advance of this report is that membranous gene-deleted rSeV significantly reduces retinal damage following gene transfer because the retina is a neuronal tissue and its regenerative capacity is limited.

It is of interest that no significant infiltration of inflammatory cells was observed over the RPE layer (in the neuroretina) in rSeV/dFdMdHN-injected eyes (Figures 3b and 3c). By contrast, the retina was extensively inflamed and underwent degeneration with rSeV/dF. We found that the deletion of all membranous genes of rSeV significantly reduced the cytopathic effect in ARPE-19 cells which are human RPE-derived cells (Figure 7a), as reported in other cell types in previous report [12]. In addition, the apoptosis of ARPE-19 cells, which was seen in rSeV/dF infection, was almost completely suppressed in use of rSeV/dFdMdHN (Figures 7b and 7c). Because RPE is part of the blood–eye barrier and limits the access of blood components to the retina [23], one reason for these histological differences might be explained by the difference of cytotoxicity to RPE. Furthermore, RPE cells have many important functions in maintaining homeostasis of the outer retina [24], and so it is necessary to retain the functions in retinal gene transfer targeting RPE. Together with the reduction of local inflammatory responses, the retinal structure is preserved in eyes treated with rSeV/dFdMdHN.

We demonstrated that the deletion of all membranous genes of rSeV resulted in the reduction of proinflammatory cytokine production and NK cell cytotoxicity; however, the cellular and molecular mechanism was not precisely elucidated in the present study. For

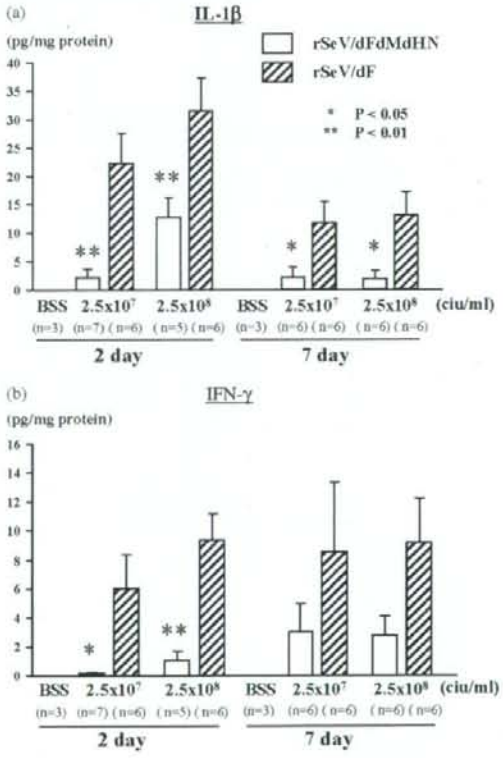

Figure 4. Assessment of proinflammatory cytokines in eyes injected with each rSeV. Protein level of IL-1β (a) and IFN-γ (b) in whole eyes was assessed on day 2 and 7 after vector injection by ELISA. The production of IL-1β and IFN-γ was reduced in rSeV/dFdMdHN-EGFP-injected eyes at each time point ($n = 5–7$ each; $^{*}p < 0.05$, $^{**}p < 0.01$, rSeV/dFdMdHN- versus rSeV/dF-injected eyes). No IL-1β or IFN-γ were detected in the BSS-injected eyes

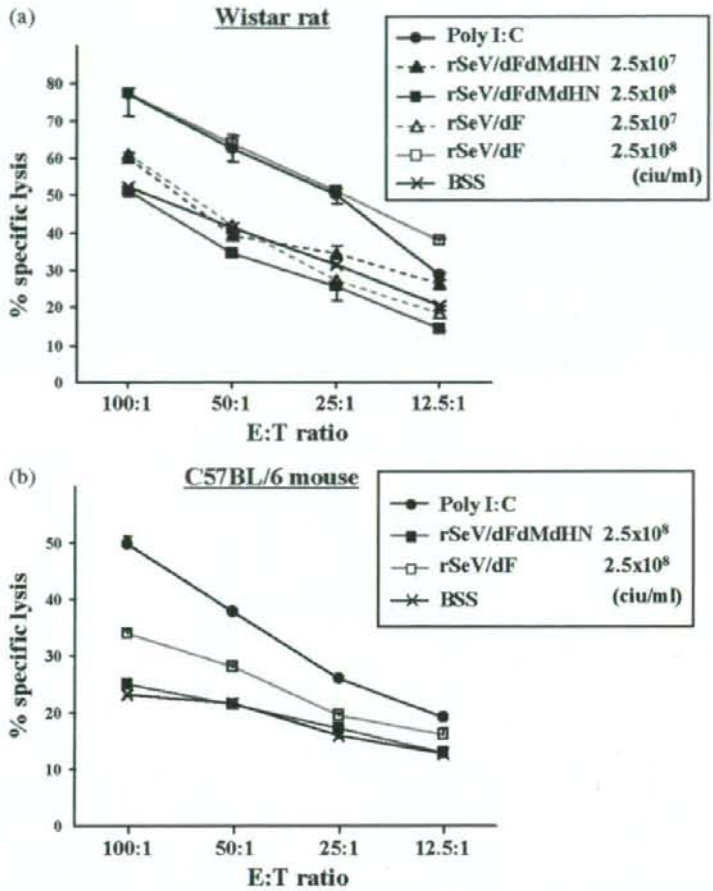

Figure 5. Assessment for NK cell activity in animals treated with each rSeV. Two days after vector injection or poly I:C administration, spleen cells were harvested from rats (a) or mice (b) treated with BSS (×), rSeV/dF-EGFP (2.5×10^7 ciu/ml) (△), rSeV/dF-EGFP (2.5×10^8 ciu/ml) (□), rSeV/dFdMdHN-EGFP (2.5×10^7 ciu/ml) (▲), rSeV/dFdMdHN-EGFP (2.5×10^8 ciu/ml) (■), or Poly I:C (●). The cytolytic function against ^{51}Cr-labelled YAC-1 targets was assessed by ^{51}Cr release. The animals treated with a high titer of rSeV/dF showed a moderate to strong increase in NK cell activity, whereas no significant increase was observed with rSeV/dFdMdHN. The data are the results from one of three similar experiments

NK cell cytotoxicity, our findings are well-supported by *in vitro* experiments indicating the recognition of the SeV HN protein by NK p44 and p46, the lysis-triggering receptors of NK cells [20,21]. For induction of proinflammatory cytokines, it is well known that host pattern-recognition receptors, such as Toll-like receptors (TLRs), have an important role after viral infection [25]. In paramyxoviruses, several studies have shown that the envelope proteins (e.g. the respiratory syncytial virus F protein and the measles virus haemagglutinin protein) bind TLR2 and TLR4, respectively, and trigger production of a variety of cytokines, such as IL-1β [26,27]. Our findings suggest that there are similar mechanisms in the recognition of SeV envelope proteins. Further studies are required to clarify this point.

The late-phase reduction of transgene expression by rSeV/dFdMdHN, illustrated in Figure 2, probably relates to the development of SeV-specific adaptive immunity, especially the CTL response. Hou *et al.* [28] reported that the CTL activity peaked on day 10 after SeV infection, and CD 8-positive T lymphocytes play a predominant role in virus clearance in the murine lung. We expected the tolerated immune responses against rSeV/dFdMdHN in ocular tissue because tolerance to foreign antigens is induced in the anterior chamber, vitreous cavity and subretinal space [14,29]; however, the present study revealed that a significant level of CTL response against SeV was induced in retinal gene transfer, as well as that seen in lung tissue [13]. In addition, the extent of CTL activity when using rSeV/dFdMdHN was stronger than that using rSeV/dF. Kast *et al.* [30] reported that the major reaction of SeV-specific CTL is directed against the NP protein. Because the gene expression by rSeV/dFdMdHN was sustained by day 4 (Figure 2), the higher CTL response may be explained by the sustained expression